Structural and electronic properties of a carbon nanotorus: Effects of delocalized and localized deformations

Lei Liu, C. S. Jayanthi, and S. Y. Wu
Department of Physics, University of Louisville, Louisville, Kentucky 40292
(Received 10 April 2001; published 27 June 2001)

The bending of a carbon nanotube is studied by considering the structural evolution of a carbon nanotorus from elastic deformation to the onset of the kinks and eventually to the collapse of the walls of the nanotorus. The changes in the electronic properties due to *delocalized* deformations are contrasted with those due to *localized* deformations to bring out the subtle issue underlying the reason why there is only a relatively small reduction in the electrical conductance in the former case even at large bending angles, while there is a dramatic reduction in the conductance in the latter case at relatively small bending angles.

DOI: 10.1103/PhysRevB.64.033412 PACS number(s): 72.80.Rj, 71.20.Tx

There have been several studies on the mechanical properties of carbon nanotubes[1] and on the interplay between the mechanical deformation and the electrical properties of single-wall nanotubes (SWNT).[2–13] Both experimental[2,3] and theoretical[4–7] studies seem to indicate that bending of the nanotubes induces only a small conductance change even at relatively large bending angles[7] (up to $\alpha = 45°$, where α is the angle between the direction tangential to the end of the tube and the unbent axis) unless the nanotubes fracture or the metal-tube contacts are perturbed.[3] Bending involved in these studies is caused by a mechanical deformation under forced confinement of the ends of the tube.[8] In this situation, the deformation induced by the bending can be viewed as a delocalized (extended) deformation. Very recently, we carried out an in-depth study, both theoretically and experimentally, of the effects of a localized mechanical deformation of a metallic SWNT induced by the pushing action of the tip of an atomic force microscope (AFM) on the electrical properties of the tube.[9,10] We observed an *unexpected* two orders of magnitude reduction in conductance at a relatively small bending angle ($\alpha = 13°$).[10] Our theoretical study confirmed that this dramatic change in conductance is due to a reversible transition from sp^2 to sp^3 bonding configurations in the bending region adjacent to the tip.[9] Thus, it is the localized deformation induced by the pushing action of the tip that is responsible for the two orders of magnitude change in conductance. This raises the question why there is only a relatively small change in conductance even at large bending angles for delocalized deformations? In this work, we address this question by investigating the mechanical deformation of a carbon nanotorus obtained by connecting the two ends of a SWNT into a ring.

We have chosen a carbon nanotorus to study the effects of bending because in this case one can determine readily the radius of curvature, the logical quantity to characterize the degree of bending at the location of bending. In previous theoretical studies,[8,11–13] the bending of the SWNT was modeled by holding the ends of the SWNT at positions defining the angle of bending. This initial configuration was then allowed to relax to its equilibrium configuration while the two ends were kept at the initial positions. Thus, there could be some ambiguity in relating the bending angle set initially with the deformation in the bending region. Specifically, unless the arclength defining the bending region is also known, the preset bending angle cannot uniquely characterize the degree of bending. On the other hand, the radius of curvature of a carbon nanotorus is well defined. Hence, a nanotorus is ideally suited for studying the effects of delocalized deformations and can, in fact, lead to an understanding of the interplay between the mechanical deformation and electronic properties of SWNTs. Furthermore, recent experimental fabrication of rings from SWNTs (Ref. 14) and subsequent measurement of magnetoresistance[15] from some of these rings underscore the importance of understanding the interplay between the mechanical deformation and the electronic properties of a nanotorus in its own right.

To study how delocalized deformations affect the structure of a nanotube, we consider a metallic (5,5) nanotube bent into a circular form with its two ends connected to form a nanotorus of a certain radius R. The initial configuration is then relaxed to its equilibrium configuration. To obtain a nanotorus, which is uniformly and elastically deformed, one must start with a nanotube of sufficiently long length. Because of the size of the system under consideration, we used the order-N nonorthogonal tight-binding molecular dynamics[16] [$O(N)$NOTB-MD] with the NOTB Hamiltonian as given in Ref. 17. We first established that a relaxed nanotorus containing 2000 atoms is indeed under a uniform and elastic deformation. This was accomplished by first obtaining the relaxed configuration of a straight 2000-atom (5,5) nanotube, next bending it into a circular form, and finally relaxing it into its equilibrium configuration. Starting from this configuration, we studied the effects of increasing deformation by reducing the radius of the nanotorus in a quasi-continuous (step-by-step) manner. Our aim is to effectively model a continuous bending process. Thus, at each step, we removed a small segment containing two circular sections, each with 10 atoms, from the nanotorus. The maximum change in the bond length with the removal of 20 atoms was less than 0.01 Å when the two ends of the broken nanotorus were elastically reconnected. This change represents a small perturbation in the strain going from one step to the next. The configuration so obtained at each step was then relaxed to its equilibrium configuration using the $O(N)$NOTB-MD scheme. The procedure was continued from the stage of elas-

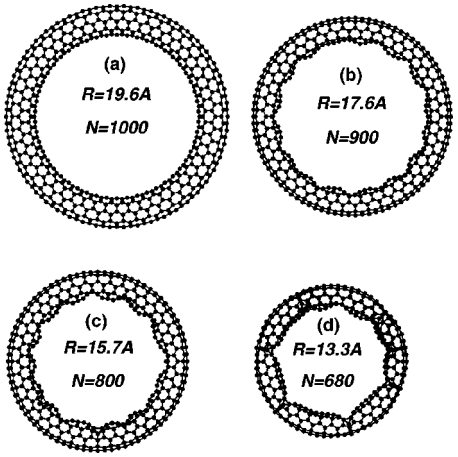

FIG. 1. Four different stages of a nanotorus under delocalized deformations. (a) Elastic deformation at $R=19.6$ Å, (b) the onset of the appearance of 16 uniformly distributed kinks at $R=17.6$ Å, (c) the merging of kinks at $R=15.7$ Å, and (d) the collapse of the walls of the nanotube at $R=13.3$ Å.

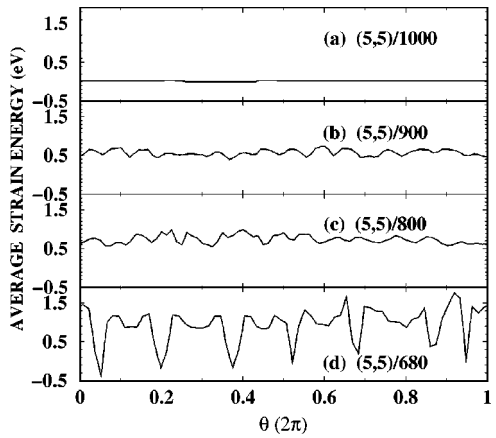

FIG. 2. The strain energy per atom averaged over the nanotorus cross section is plotted as a function of θ, where θ represents the angular position along the circumference of the torus for the four cases depicted in Fig. 1. (a) shows that the strain energy is almost uniformly distributed along the circumference (an elastically deformed torus), (b)–(c) show that the strain energy exhibit local minima at the location of kinks where the release of the strain energy occurs, while (d) shows that there is a dramatic drop in the strain energy at the locations of the collapse of the walls.

tic deformation, to the stage of the development of the kinks, and eventually to the stage of topological change in the structure in the bending region. In the present study, from a torus of sufficiently large radius of curvature (for example, from a 2000-atom torus) down to a 1000-atom torus, the deformation was found to be elastic.

We highlight the ''continuous'' process of bending by four representative configurations shown in Fig. 1. Figures 1(a)–1(d) give the equilibrium configurations obtained by the MD procedure outlined above for nanotori containing 1000 ($R=19.6$ Å), 900 ($R=17.6$ Å), 800 ($R=15.7$ Å), and 680 ($R=13.3$ Å) atoms, respectively. An examination of the structures shown in Fig. 1 reveals the following features. From Fig. 1(a), it can be seen that the nanotorus of $R=19.6$ Å is under a uniform elastic distortion, with a simple stretching on the outer side and simple compression on the inner side. It gives an example of a SWNT under elastic deformation and indicates that the (5,5) SWNT is still only elastically deformed at a radius of curvature R of 19.6 Å under a uniform deformation. As R is reduced to 17.6 Å with a corresponding increase in the mechanical deformation, the structural distortion is characterized by the appearance of 16 almost uniformly distributed kinks along the inner (compression) side of the nanotorus [see Fig. 1(b)]. The appearance of the kinks is attributable to the release of the strain energy at a critical radius of curvature of about 17.6 Å in the bending region. Further reduction of R with the accompanying increase in the distortion brings about the reduction of the number of kinks while enhancing the release of the strain energy at the kinks as exemplified in Fig. 1(c). Finally when R reaches 13.3 Å, the collapsing of the inner and outer walls of the nanotorus occurs [see Fig. 1(d)], signaling a topological change in the structure in the region of collapse at a critical radius of curvature of about 13.3 Å. During the simulation of the ''continuous'' bending, extreme care was exercised in monitoring the onset of the fundamental structural change. However, due to the discrete nature of the removal of small segment from the nanotorus, there is a built-in degree of uncertainty in pinning down precisely the radius of curvature when a certain structural change occurs. Hence the numbers given above as critical radii of curvature for various structural changes are approximate.

To explore in more detail the structural changes induced by a delocalized deformation, we calculated the average strain energy per atom over each section (containing 10 atoms) of the relaxed nanotorus. The angular location of the section is denoted by θ with $\theta=0$ along the positive horizontal direction and increasing in the clockwise direction. The total energy of the nanotorus can be expressed as the sum of the site energy of atoms in the nanotorus within the framework of a NOTB Hamiltonian.[18] The strain energy of an atom at a given site in the relaxed (5,5) nanotorus is defined as the energy difference between the energy of the atom at that site and the energy per atom for the relaxed ideal straight (5,5) nanotube. The average strain energy per atom for a given section is simply the average of the strain energy for the atoms in that section. In Fig. 2, the average strain energy per atom for the four nanotori is plotted against θ. For the nanotorus of $R=19.6$ Å, the strain energy is small and uniform along the entire torus, indicating that the torus is under simple elastic deformation. When R is reduced to 17.6 Å, the average strain energy along the torus is increased substantially and 16 local minima appear in the plot at the angles where the kinks are located, a clear indication of the release of the strain energy at the kinks. When R is reduced to 15.7 Å (800 atoms), there is only a slight increase in the average strain energy at locations near the kinks with enhanced local minima. However, when R reaches 13.3 Å, pronounced local minima appear at locations precisely matching where collapsing of the walls occurs. These enhanced local minima actually accompany a substantial increase in the average strain energy per atom along the torus.

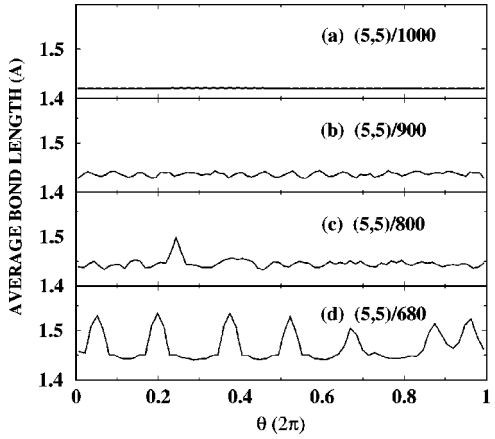

FIG. 3. The average bond length vs θ. (a) The average bond length is close to 1.42 Å, the sp^2 bond length of the graphene sheet, (b)–(c) the average bond length is larger than case (a), and (d) the average bond length exhibits local maxima (at the collapsed region) with values close to 1.54 Å, the sp^3 bond length of diamond.

A side-by-side comparison of Figs. 2 and 3, where the average bond length is plotted vs θ , is even more illuminating. While the average bond length along the torus is somewhat longer than the bond length of the ideal straight (5,5) nanotube for the three nanotori with the radius of 19.6 Å, 17.6 Å, and 15.7 Å, respectively, the average bond length for the nanotorus with the radius 13.3 Å at the locations of wall-collapsing is 1.53 Å, substantially longer than the bond length of 1.42 Å for the sp^2 bonding configuration in the ideal straight (5,5) nanotube and in fact close to the bond length of 1.54 Å for the sp^3 bonding configuration in diamond. This is the signature of the topological change in the structure for the 680-atom nanotorus in the region of wall collapsing. Further confirmation of this picture can be seen from Fig. 4 where the average coordination number is plotted vs θ . It can be seen that the average coordination number at the locations of wall collapsing for the nanotorus of radius

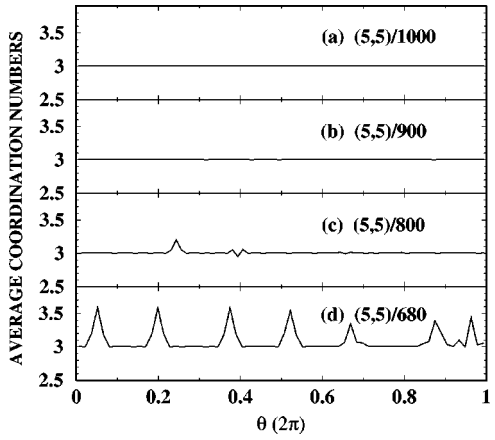

FIG. 4. The average coordination number vs θ. The average coordination number increases from a constant value of 3 in (a), as in sp^2 bonding, to a value of about 3.6 at the local maxima in (d), close to the value of 4 as in sp^3 bonding.

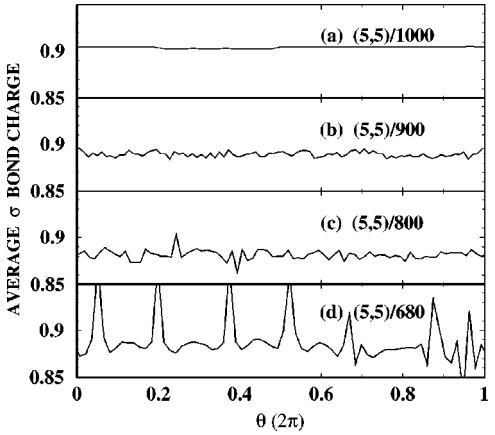

FIG. 5. The average σ bond charge vs θ. While the average σ bond charge decreases slightly in (a)–(c), (d) shows a dramatic increase in the bond charge at the collapsed regions of the wall.

13.3 Å is about 3.6, close to the 4-coordinated sp^3 configuration, while the coordination number along the circumference of the first three nanotori is close to 3, the coordination number for the sp^2 configuration. Thus, our investigation has succinctly established the effects on the structure of a SWNT due to a delocalized deformation, namely, from a simple elastic distortion for large radii of curvature, to the appearance of kinks at a critical radius of curvature of about 17.6 Å, followed by the collapse of the walls involving the transition from the sp^2 configuration to the sp^3 configuration at a critical radius of curvature of about 13.3 Å for the (5,5) SWNT. Within the framework of the nanotorus, one may set up a benchmark for comparison with previous studies. Specifically, referring to Fig. 1(b), since there are 16 uniformly distributed kinks, one may estimate the critical angle for the appearance of the kink under a delocalized deformation as $\alpha_K=\frac{1}{2}(2\pi/16)\simeq 11°$. Similarly, from Figs. 2(d), 3(d), and 4(d), corresponding to the 680-atom case, one may surmise that there should be seven equivalent pronounced peaks or valleys at the locations of wall collapsing along the circumference. Hence, the critical bending angle for the transition from sp^2- to sp^3-bonding configuration under a delocalized deformation can be estimated as $\alpha_C=\frac{1}{2}(2\pi/7)\simeq 26°$.

To understand the interplay between the mechanical deformation and the electronic properties, we calculated the average σ-bond charge and the average π-bond charge per atom following the procedures given in Refs. 9,18. The results are shown in Figs. 5 and 6, respectively. It can be seen that, for the first three nanotori, there is only some slight reduction of both the σ- and the π-bond charges along the circumference associated with the bond stretching as the nanotorus is under increasing strain. Thus, there is no basic change in the nature of electronic structure and hence no significant change in conductance is expected for a SWNT under delocalized deformations up to a radius of curvature of about 13.3 Å. However when the strain reaches a critical value such that wall collapsing occurs ($R\leqslant 13.3$ Å), there is a substantial increase in the σ-bond charge and a pronounced decrease in the π-bond charge at the locations where the walls collapse, a reflection of the transition from the sp^2

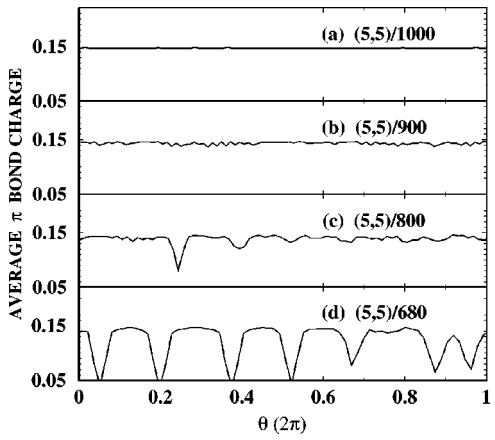

FIG. 6. The average π bond charge vs θ. While the average π-bond charge decreases slightly in (a)–(c), (d) shows a dramatic decrease in the bond charge at the collapsed regions of the wall.

bonding configuration to the sp^3 bonding configuration. (It should be noted that this is precisely the mechanism that comes into play for a SWNT under a localized deformation at relatively small bending angles.[9,10]) The π electrons are delocalized and mainly responsible for conduction while the σ electrons are localized. Therefore one might expect that the dramatic reduction of the π-bond charge and substantial increase in the σ-bond charge will lead to a substantial reduction in conductance for a nonlocalized deformation for $R \leqslant 13.3$ Å (i.e., $\alpha \geqslant 26°$). We, therefore, calculated the electrical conductance corresponding to the wall-collapsing case ($R=13.3$ Å) by using the Landauer's formula.[9,19] We chose the segment of the nanotorus containing 12 sections that includes the wall collapsing in its center as our sample and connected it to ideal (5,5) SWNT leads. We obtained a conductance of $0.5G_0$ ($G_0=2e^2/h$) at the Fermi energy, a factor of 4 reduction from the ideal straight (5,5) nanotube, consistent with previous calculations.[12] This is, however, in dramatic contrast to the case of a localized deformation, where a small bending angle induces a two orders of magnitude reduction.[9,10] We examined this issue by referring to the half width of the pronounced peak in the σ-bond charge (Fig. 5) and that of the deep valley in the π-bond charge (Fig. 6) for the 680-atom torus. It can be seen that both are about 0.24 rad, indicating that the transition from the sp^2- to the sp^3-bonding configuration only extends to a region of about 3 Å. It should be noted that the transition from the sp^2- to sp^3-bonding configuration induced by the manipulation of an AFM tip extends to a region of ~ 12 Å at a small bending angle of 15° (see Fig. 3 in Ref. 9). The comparison explains why the reduction in conductance is relatively small even at large bending angles under a delocalized deformation while a two orders of magnitude reduction in conductance is observed under a localized deformation.

The present study contrasts our previous studies[9,10] on the effects of localized deformations on a SWNT. In particular, it brings out the important point that the deciding factor for the dramatic reduction of the conductance of metallic SWNTs is the combined effect of the transition from the sp^2- to sp^3-bonding configuration and the extent of the bending region where the transition occurs. With this study, we have now established a complete picture of the interplay between the mechanical deformation, be it a delocalized deformation or a localized deformation, and the electronic properties of SWNTs. Our findings should provide useful guidelines for the design of nanoscale electromechanical devices based on SWNTs.

This work was supported by the the NSF (Grant No. DMR-9802274) and the U.S. DOE (Grant No. DE-FG02-00ER45832). We acknowledge that this work was carried out on the HP-Exemplar computer at the University of Kentucky. We thank Professor E. Kaxiras for his useful comments.

[1] B.I. Yakobson, C.J. Brabec, and J. Bernholc, Phys. Rev. Lett. **76**, 2511 (1996).
[2] A. Bezryadin, A.R.M. Verschueren, S.J. Tans, and C. Dekker, Phys. Rev. Lett. **80**, 4036 (1998).
[3] S. Paulson, M.R. Falvo, N. Snider, A. Helser, T. Hudson, A. Seeger, R.M. Taylor, R. Superfine, and S. Washburn, Appl. Phys. Lett. **75**, 2936 (1999).
[4] V.H. Crespi, M.L. Cohen, and A. Rubio, Phys. Rev. Lett. **79**, 2093 (1997).
[5] C.L. Kane and E.J. Mele, Phys. Rev. Lett. **78**, 1932 (1997).
[6] M.B. Nardelli, B.I. Yakobson, and J. Bernholc, Phys. Rev. Lett. **81**, 4656 (1998).
[7] A. Rochefort, F. Lesage, D.R. Salahub, and P. Avouris, cond-mat/9904083 (unpublished).
[8] S. Iijima, C. Brabec, A. Naiti, and J. Bernholc, J. Chem. Phys. **104**, 2089 (1996).
[9] L. Liu, C.S. Jayanthi, M. Tang, S.Y. Wu, T.W. Tombler, C. Zhou, L. Alexseyev, J. Kong, and H. Dai, Phys. Rev. Lett. **84**, 4950 (2000).
[10] T.W. Tombler, C. Zhou, L. Alexseyev, J. Kong, H. Dai, L. Liu, C.S. Jayanthi, M. Tang, and S.Y. Wu, Nature (London) **405**, 769 (2000).
[11] M. Nardelli, Phys. Rev. B **60**, 7828 (1999).
[12] M. Nardelli and J. Bernholc, Phys. Rev. B **60**, 16 338 (1999).
[13] A. Rochefort, D.R. Salahub, and P. Avouris, Chem. Phys. Lett. **297**, 45 (1998).
[14] R. Martel, H.R. Shea, and P. Avouris, Nature (London) **398**, 299 (1999).
[15] H.R. Shea, R. Martel, and Ph. Avouris, Phys. Rev. Lett. **84**, 4441 (2000).
[16] C.S. Jayanthi, S.Y. Wu, J. Cocks, N.S. Luo, Z.L. Xie, M. Menon, and G. Yang, Phys. Rev. B **57**, 3799 (1998).
[17] M. Menon, K.R. Subbaswamy, and M. Sawtarie, Phys. Rev. B **48**, 8398 (1993).
[18] D. Alfonso, S.Y. Wu, C.S. Jayanthi, and E. Kaxiras, Phys. Rev. B **59**, 7745 (1999).
[19] S. Datta, *Electronic Transport in Mesoscopic Systems* (Cambridge University Press, Cambridge, 1995).